

Toward precise Q_{EC} values for the superallowed $0^+ \rightarrow 0^+$ β decays of $T = 2$ nuclides: The masses of ^{20}Na , ^{24}Al , ^{28}P , and ^{32}Cl

C. Wrede,^{1,2,*} J. A. Clark,^{2,3} C. M. Deibel,^{2,3,4} T. Faestermann,⁵ R. Hertenberger,⁶ A. Parikh,⁵ H.-F. Wirth,⁶ S. Bishop,⁵
A. A. Chen,^{7,8} K. Eppinger,⁵ A. García,¹ R. Krücken,⁵ O. Lepyoshkina,⁵ G. Rugel,⁵ and K. Setoodehnia⁷

¹Department of Physics, University of Washington, Seattle, Washington 98195, USA

²Wright Nuclear Structure Laboratory, Yale University, New Haven, Connecticut 06520, USA

³Physics Division, Argonne National Laboratory, Argonne, Illinois 60439, USA

⁴Joint Institute for Nuclear Astrophysics, Michigan State University, East Lansing, Michigan 48824, USA

⁵Physik Department E12, Technische Universität München, D-85748, Garching, Germany

⁶Fakultät für Physik, Ludwig-Maximilians-Universität München, D-85784, Garching, Germany

⁷Department of Physics and Astronomy, McMaster University, Hamilton, Ontario L8S 4M1, Canada

⁸DFG Cluster of Excellence Origin and Structure of the Universe, Technische Universität München, D-85748, Garching, Germany

(Received 5 March 2010; published 21 May 2010)

High-precision measurements of superallowed $0^+ \rightarrow 0^+$ β decays of $T = 2$ nuclides such as ^{20}Mg , ^{24}Si , ^{28}S , and ^{32}Ar can contribute to searches for physics beyond the standard model of particle physics if the Q_{EC} values are accurate to a few keV or better. As a step toward providing precise Q_{EC} values for these decays, the ground-state masses of the respective daughter nuclei ^{20}Na , ^{24}Al , ^{28}P , and ^{32}Cl have been determined by measuring the ($^3\text{He}, t$) reactions leading to them with the $^{36}\text{Ar}(^3\text{He}, t)^{36}\text{K}$ reaction as a calibration. A quadrupole-dipole-dipole-dipole (Q3D) magnetic spectrograph was used together with thin ion-implanted carbon-foil targets of ^{20}Ne , ^{24}Mg , ^{28}Si , ^{32}S , and ^{36}Ar . The masses of ^{20}Na and ^{32}Cl are found to be in good agreement with the values from the 2003 Atomic Mass Evaluation (AME03) [G. Audi, A. H. Wapstra, and C. Thibault, *Nucl. Phys. A* **729**, 337 (2003)], and the precision has been improved by a factor of 6 in both cases. The masses of ^{24}Al and ^{28}P are found to be higher than the values from AME03 by 9.5 keV (3.2σ) and 11.5 keV (3.6σ), respectively, and the precision has been improved by a factor of 2.5 in both cases. The new ^{32}Cl mass is used together with the excitation energy of its lowest $T = 2$ level and the mass of ^{32}Ar to derive an improved superallowed Q_{EC} value of 6087.3(22) keV for this case. The effects on quantities related to standard-model tests including the β - ν correlation coefficient a and the isospin-symmetry-breaking correction δ_C are examined for the $A = 32$ case.

DOI: [10.1103/PhysRevC.81.055503](https://doi.org/10.1103/PhysRevC.81.055503)

PACS number(s): 21.10.Dr, 07.75.+h, 24.80.+y, 27.30.+t

I. INTRODUCTION

As radioactive ion-beam facilities push toward the nucleon drip lines, precision β -decay measurements of very neutron-deficient isotopes are becoming accessible. β -decay schemes increase in complexity as the proton drip line is approached, and this complicates the analysis of such experiments. It is therefore important to improve basic information, such as ground-state masses, on unstable nuclides that appear in the decay cascades. For example, the superallowed $0^+ \rightarrow 0^+$ β decays of $T = 2$ nuclides have the potential to contribute to tests of the standard model of particle physics (SM) in at least two ways: via searches for scalar currents using the β - ν correlation, and via checks of isospin-symmetry-breaking corrections to ft values that are used to test unitarity of the Cabibbo-Kobayashi-Maskawa (CKM) matrix. To date, these tests using $T = 2$ β decays have only been realized in the case of ^{32}Ar [1,2], and the results are being revised as basic nuclear data are refined [2–6].

Nuclear β decay is mediated by the W^\pm vector boson in the SM. Scalar-current contributions could result from the exchange of a particle beyond the SM such as a leptoquark or a charged Higgs boson [1]. Such scalar currents may be sought

by measuring the angular correlation between the emitted leptons and comparing it with the SM prediction. For pure Fermi decays, the angular correlation coefficient a is unity in the SM. For decays of $T = 1$ nuclides near the valley of β stability, the $e^+ - \nu_e$ correlation can be measured by trapping the parent nuclide using electromagnetic fields and detecting the positron and the recoiling nucleus in coincidence, thereby fully constraining the kinematics and allowing reconstruction of the neutrino momentum [7]. The $T = 2$ decays lie farther from stability. As a result, the isobaric-analog daughter state is often proton unbound, and this allows the $e^+ - \nu_e$ correlation to be measured by a different means: all of the necessary kinematic information on the superallowed decay is contained in the *shape* of the corresponding β -delayed proton-energy distribution. This distribution can be measured to determine the quantity \tilde{a} , which is identical to a for vanishing Fierz interference [1,8]. The accuracy of this method is dependent on the accuracy of the mass-excess difference between the parent atom and daughter level in the decay, Q_{EC} , which must be known to a few keV or better to compete with present limits on \tilde{a} [1,7], and is determined by independent measurements.

The CKM quark-mixing matrix is unitary in the SM, and thus violations of unitarity would indicate the need for physics beyond the SM. Currently the sum of the squares of the top-row elements V_{ud} , V_{us} , and V_{ub} provides the best experimental test of CKM unitarity and verifies the SM

*Corresponding author: wrede@uw.edu

prediction [8]. Corrected $\mathcal{F}t \equiv ft(1 - \delta_C)(1 + \delta_R)$ values for superallowed $0^+ \rightarrow 0^+$ β decays of $T = 1$ nuclides impose the most stringent constraints on the largest of these elements, V_{ud} [8]. Experimental determinations of the half-lives, Q_{EC} values, and superallowed branchings for the $T = 1$ decays have become sufficiently precise that uncertainties in the theoretical isospin-symmetry-breaking corrections δ_C need to be carefully considered [8–13]. The $T = 2 0^+ \rightarrow 0^+$ β decays are expected to have larger δ_C because of the high density of states near the daughter levels. Precision measurements of the ft values for the $T = 2$ β decays can therefore provide valuable tests of isospin-symmetry-breaking calculations. A pioneering test of this kind has recently been carried out for the case of ^{32}Ar where the experimental value $\delta_C^{\text{exp}} = 2.1(8)\%$ was found to agree with the theoretical value $\delta_C^{\text{th}} = 2.0(4)\%$ [2], but the test would evidently benefit from a reduction in the experimental uncertainty. Among several contributing uncertainties, the Q_{EC} value of the superallowed decay directly affects δ_C^{exp} and should be accurate to better than a few keV to provide a more meaningful test of the calculation. The same is true for every $T = 2$ case considered in the present work.

The desired accuracy has not yet been achieved for the Q_{EC} values of the $T = 2$ decays of ^{20}Mg , ^{24}Si , ^{28}S , or ^{32}Ar . It is the purpose of the present work to advance experimental information on the mass excesses of the corresponding daughter levels: the lowest $T = 2$ levels in ^{20}Na , ^{24}Al , ^{28}P , and ^{32}Cl . Our strategy is to measure the ground-state masses of these nuclides with the expectation that the γ decays of the $T = 2$ levels will be measured in the future to determine the total branchings of the superallowed decays, and to provide precise excitation energies. In the case of ^{32}Cl the excitation energy has already been measured to 0.4 keV in this manner [2]. All of the $T = 2$ daughter levels under consideration are proton unbound by several MeV, but their proton decays are isospin forbidden. This narrows the proton partial widths so that the γ -decay branches are expected to be non-negligible, as seen in the case of ^{32}Cl [2].

In the most recent Atomic Mass Evaluation (AME03) [14], the mass excesses of ^{20}Na , ^{24}Al , ^{28}P , and ^{32}Cl are assigned uncertainties of 7, 2.8, 3, and 7 keV, respectively. The corresponding recommended values are therefore not sufficiently precise for SM tests, and there is also reason to believe they may be inaccurate. They are based almost entirely on (p, n) reaction threshold measurements [15–17], and a number of systematic effects can introduce errors to the extraction of Q values and masses from (p, n) thresholds [15, 18]. For example, the work of Ref. [15] was focused on accelerator calibration and did not declare measurements of these quantities. Nevertheless, all of the AME03 mass values in question are calibrated against the $^{24}\text{Mg}(p, n)^{24}\text{Al}$ threshold from Ref. [15]. Moreover, these masses have been adjusted many times by amounts as large as ≈ 10 keV, since the initial measurements (e.g., Refs. [14, 18]). Recently, a direct measurement [19] of the energy of the lowest-lying resonance in the $^{23}\text{Mg}(p, \gamma)^{24}\text{Al}$ reaction was found to be inconsistent with the energy derived using the mass excesses from AME03 [14] together with the excitation energies from Refs. [20, 21]. This result points to a potential problem with the AME03 mass of ^{24}Al that would affect the masses of ^{20}Na , ^{28}P , and ^{32}Cl .

Evidently, new measurements are needed to provide accurate and precise masses. We have determined the ground-state masses of ^{20}Na , ^{24}Al , ^{28}P , and ^{32}Cl by measuring the $(^3\text{He}, t)$ reactions leading to these nuclides with the $^{36}\text{Ar}(^3\text{He}, t)^{36}\text{K}$ reaction as a calibration.

II. EXPERIMENT

The experiment was carried out at the Maier-Leibnitz-Laboratorium (MLL) of the Ludwig-Maximilians-Universität and the Technische Universität München during November 2009 following preliminary measurements at the Wright Nuclear Structure Laboratory (WNSL) of Yale University during December 2007. The present article will focus on the measurements at MLL because they are more precise and because they included a calibration standard.

At MLL, a 32-MeV, ≈ 400 -enA $^3\text{He}^{2+}$ beam was produced using an electron cyclotron resonance (ECR)-like ion source [22] and an MP tandem Van de Graaff accelerator. The beam was first tuned through a 1×3 mm extractable collimator at the target position and was then incident upon thin, ion-implanted targets of ^{20}Ne , ^{24}Mg , ^{28}Si , ^{32}S , and ^{36}Ar that are described in the following paragraph. Beam current was integrated using a Faraday cup at 0° . A quadrupole-dipole-dipole-dipole (Q3D) magnetic spectrograph was used to momentum-analyze the light reaction products that passed through a 6.25-msr rectangular entrance aperture with horizontal and vertical angular dimensions of $\pm 1.37^\circ$ and $\pm 3.74^\circ$ in the laboratory frame, respectively. The spectrograph was set to focus tritons corresponding to the low-lying levels of the product nuclides of interest onto a gas proportional counter backed by a scintillator. These detectors recorded the position, energy loss, and residual energy of both tritons and deuterons providing clean particle identification, and position resolution much better than the intrinsic resolution of the spectrograph ($\Delta E/E \approx 2 \times 10^{-4}$) [23, 24]. Measurements were made with the spectrograph positioned at two separate angles (10° and 20° in the laboratory frame) to kinematically identify peaks and check the reproducibility of the results. The targets were cycled in various orders, and runs of 1–2 hours in duration were taken over a total of 6 days. The similar Q values of these $(^3\text{He}, t)$ reactions allowed them to be measured together with identical settings and a common calibration. The multipole element of the Q3D spectrograph [25] was set to compensate for the kinematic broadening of the $^{28}\text{Si}(^3\text{He}, t)$ reaction and was therefore not optimum for the other reactions.

The preliminary measurements at WNSL were made with available targets that included $< 1 \mu\text{g}/\text{cm}^2$ of ^{20}Ne implanted in a thin carbon foil, a heavily oxidized natural Mg foil supported by parylene backing, a self-supporting Si foil, and CdS evaporated onto a natural carbon foil. A 32-MeV $^3\text{He}^{2+}$ beam was provided by an extended stretched transuranium (ESTU) tandem Van de Graaff accelerator, and an Enge split-pole magnetic spectrograph was positioned at a laboratory angle of 10° with a position-sensitive detector backed by a scintillator at the focal plane. With the exception of the relatively thin ^{20}Ne target, the target thicknesses were 150 to 300 $\mu\text{g}/\text{cm}^2$. Despite dedicated elastic-scattering measurements using an 8-MeV ^4He beam to characterize the targets, the ≈ 3 keV

uncertainties in the relative Q values of the ($^3\text{He}, t$) reactions were dominated by uncertainties in target thickness and profile. To improve this situation for the measurement at MLL, targets of ^{20}Ne , ^{24}Mg , ^{28}Si , ^{32}S , and ^{36}Ar were prepared at the Center for Experimental Nuclear Physics and Astrophysics of the University of Washington by implanting $\approx 4 \mu\text{g}/\text{cm}^2$ of each of these ions into separate $30 \mu\text{g}/\text{cm}^2$ natural-carbon foils. For each target, four or six layers of material were deposited at different depths inside the foil by implanting at two or three different energies in equal amounts through each side of the foil to produce a depth distribution of implanted material that was symmetric about the middle of the foil. The total number of ions implanted was measured by integrating the electrical current on the foil, and transverse uniformity was achieved by magnetically rastering the ion beam. This target-preparation technique produced targets that were nearly identical to each other in thickness and profile despite the unique chemistry of each element. For example, it prevented excessive oxidation in the case of Mg, eliminated the usual need for a chemical-compound target in the case of S, and made the noble-gas element targets commensurate with the others. In addition, this technique produced isotopically pure targets, eliminating any background that would otherwise be present from the isotopes $^{21,22}\text{Ne}$, $^{25,26}\text{Mg}$, $^{29,30}\text{Si}$, $^{33,34,36}\text{S}$, and $^{38,40}\text{Ar}$. Employing such similar targets minimized the systematic uncertainties associated with target characterization. The target preparation was a key part of these measurements and will be described in more detail in a technical publication [26].

III. ANALYSIS

The masses of ^{20}Na , ^{24}Al , ^{28}P , and ^{32}Cl were determined by measuring the momenta of tritons emitted from the ($^3\text{He}, t$) reactions leading to the ground and low-lying excited states of these nuclides with respect to the relatively well-known momenta of tritons from the $^{36}\text{Ar}(^3\text{He}, t)^{36}\text{K}$ reaction.

Histograms of triton and deuteron positions at the focal plane were produced for each run by sorting the data through particle-identification gates in two-dimensional spectra. It became evident after the first 24 hours of the experiment that the horizontal position of the beam on the target was drifting at an average rate of ≈ 1 mm per day. The drift was subsequently controlled by checking the beam tune through the collimator about three times per day. Nevertheless, this effect continued to produce a significant systematic drift in focal-plane position that presented a direct systematic error to the experiment. We expect the shift in focal-plane position from this effect to be equal for tritons and deuterons, because the paths of these particles through the spectrograph should be displaced equally based on an equal displacement of the initial interaction point. Peaks from ($^3\text{He}, d$) reactions common to every target were used to measure the displacement for every run relative to an arbitrary central value. These displacements were found to be consistent with the displacements of the triton spectra in the corresponding runs, confirming that the displacements were due to drifts in beam position. To correct for this effect, each triton spectrum was shifted to conform

to a common arbitrary reference based on the deuteron shifts. Typical shifts were roughly zero to three channels in magnitude, corresponding to roughly 0 to 1.8 keV in triton energy. The maximum shift imposed for any single run was six channels. Following the shifting procedure, runs taken with a particular target at a particular angle were summed to produce a single spectrum. The systematic uncertainty associated with shifting each spectrum to the central value and summing was estimated to be 0.5 channels. To ensure that normal statistics could be applied to each bin when fitting the spectra, the 10° and 20° triton spectra were rebinned by factors of 2 and 4, respectively.

Although backgrounds in the triton spectra were not a serious problem, they were accounted for. The predominant background in every spectrum was from the $^{13}\text{C}(^3\text{He}, t)$ reaction, which produced a continuum and one discernible broad peak from the $E_x = 11.86$ MeV ($\Gamma = 380$ keV) level in ^{13}N [27]. Runs were taken at each angle with an enriched $27 \mu\text{g}/\text{cm}^2$ ^{13}C target to measure the background, which was normalized and subtracted from each spectrum. The background-subtracted spectra from the 10° measurements are shown in Fig. 1.

Peaks were fit with Gaussian functions from which centroids and widths were extracted. Average full width at half maximum (FWHM) energy resolution was ≈ 13 keV at 10° and ≈ 18 keV at 20° but depended on the mass of the target nuclide as discussed later in this section. Identifying each peak was trivial thanks to the well-known low-lying level structure of each product nuclide, the roughly known Q value of each reaction, and the kinematic shifts measured from 10° to 20° . Peaks corresponding to the ground and well-known excited states of each product nuclide (Table I) were used in the mass determinations together with the known masses of the other nuclides involved in the reactions (Table II). For the cases of ^{20}Na , ^{24}Al , ^{28}P , and ^{36}K , at least two peaks were suitable, reducing the uncertainty that would result from using a single peak per nuclide. At each angle, a second-degree polynomial least-squares fit was used to relate the triton focal-plane position to the effective radius of the triton path through the dipole magnets. The input data were weighted by the statistical uncertainties in the peak centroids and the uncertainties in the adopted excitation energies. The fits effectively related focal-plane position to triton momentum via magnetic rigidity under the assumption of a constant magnetic field (the magnetic field was regulated). Nominal nuclear masses were incorporated as initial inputs for every reaction except for the $A = 36$ case, which provided a calibration standard. The masses of ^{20}Na , ^{24}Al , and ^{28}P were then allowed to vary in the fits until the χ^2/ν statistics were minimized at values of 19.7/8 and 7.8/7 at 10° and 20° , respectively.¹

¹The relatively large χ^2/ν at 10° could be attributed to angular-distribution effects (discussed below), slight departures of the peak shapes from Gaussian, or inaccurate adopted data. Inflation by factors of $\sqrt{\chi^2/\nu}$ of the uncertainties in the momenta extracted from the 10° fit were applied, but the magnitudes of the corresponding increases in the mass uncertainties were very small compared to other uncertainties (Table III).

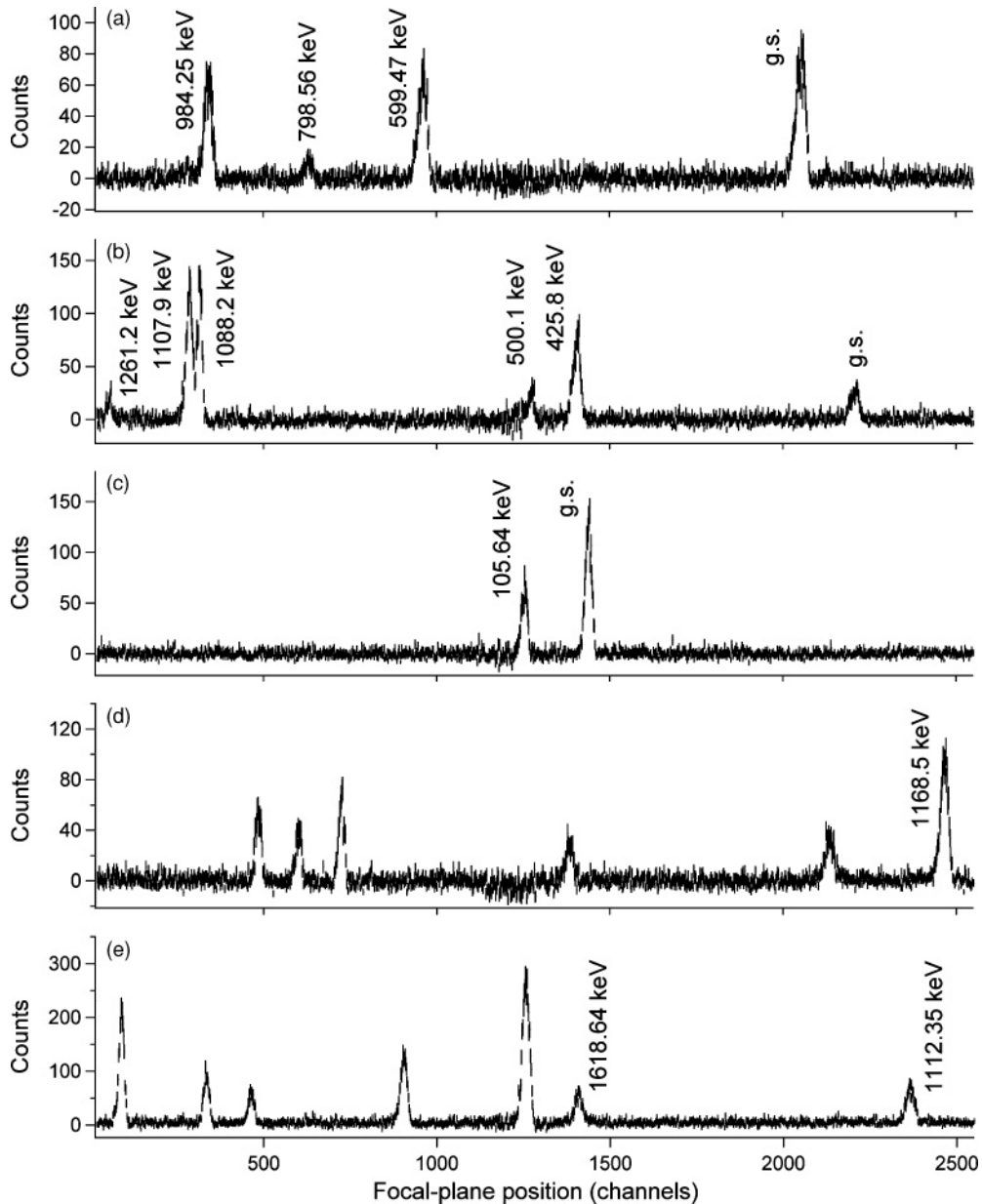


FIG. 1. Q3D focal-plane position spectra of tritons from the $({}^3\text{He}, t)$ reactions leading to (a) ${}^{20}\text{Na}$, (b) ${}^{24}\text{Al}$, (c) ${}^{28}\text{P}$, (d) ${}^{32}\text{Cl}$, and (e) ${}^{36}\text{K}$, acquired using a beam energy of 32 MeV at $\theta_{\text{lab}} = 10^\circ$. The data are sorted into bins comprised of two channels. For each bin, the datum is plotted as a vertical line with a length that spans the standard deviation. Increases in fluctuations between channels 1100 and 1300 are due to the subtraction of background from the ${}^{13}\text{C}({}^3\text{He}, t){}^{13}\text{N}$ reaction. Peaks used in the analysis are labeled by “g.s.” for ground states and the excitation energy for excited states (Table I).

This procedure yielded measures of the ground-state masses of ${}^{20}\text{Na}$, ${}^{24}\text{Al}$, and ${}^{28}\text{P}$ at each angle. The centroid of a single peak corresponding to $E_x = 1168.5(2)$ keV in ${}^{32}\text{Cl}$ was used together with the final fits to determine the ground-state mass of ${}^{32}\text{Cl}$ at each angle. This level alone was used for ${}^{32}\text{Cl}$ because the kinematics did not allow inclusion of the ground-state peak on the focal plane together with the other ground-state peaks, and the excitation energies of other ${}^{32}\text{Cl}$ peaks observed are not known with sufficiently high precision.

Many uncertainties had to be considered in arriving at a final uncertainty for each mass measurement. Although it

is difficult to completely decouple these uncertainties from each other, they were divided roughly into two categories: (I) uncertainties that shift the masses in the same direction by the same magnitude at both angles and (II) uncertainties that are unique to the measurements at each angle.

Category I comprises uncertainties in adopted data that were used for calibration and uncertainties in total target thicknesses. The uncertainty in the ground-state mass of ${}^{36}\text{K}$ is 390 eV [38]. The two excited states of ${}^{36}\text{K}$ that were used as calibration standards have each been measured twice to uncertainties ≤ 400 eV, but the measurements are

TABLE I. Adopted excitation energies for peaks used as input to the focal-plane fits.

Nuclide	E_x (keV)	Refs.
^{20}Na	g.s.	
^{20}Na	599.47(5)	[28]
^{20}Na	798.56(6)	[28]
^{20}Na	984.25(10)	[29,30]
^{24}Al	g.s.	
^{24}Al	425.8(1)	[27,31]
^{24}Al	500.1(1)	[21]
^{24}Al	1088.2(2)	[21]
^{24}Al	1107.9(1)	[21]
^{24}Al	1261.2(3) ^a	[21]
^{28}P	g.s.	
^{28}P	105.64(10)	[27,32]
^{32}Cl	1168.5(2) ^b	[27,33]
^{36}K	1112.35(45) ^c	[34–36]
^{36}K	1618.64(72) ^c	[34–36]

^aNot used for 20° data: off focal-plane detector.

^bNot used for input to the focal-plane fits; only used for output.

^cWeighted average with inflated uncertainties; see text.

somewhat inconsistent [34–36]. Therefore a weighted average was taken, and the uncertainties were inflated to account for the inconsistencies [39]. The average values adopted were $E_x = 1112.35(45)$ and $1618.64(72)$ keV. Used together, the excitation energies of these two levels contribute a total uncertainty of 382 eV. Uncertainties in adopted data for excitation energies of the other product nuclides were ≤ 200 eV (Table I). An estimate of the uncertainty due to absolute target thickness can be made based on the C-foil-thickness specifications ($30 \pm 3 \mu\text{g}/\text{cm}^2$) of the commercial supplier.² However, yields in the ($^3\text{He}, d$) peaks resulting from the carbon foils showed that the relative thicknesses of the C foils were actually much closer than this uncertainty would

²Arizona Carbon Foil Company, Tucson, AZ 85719, USA.

TABLE II. Adopted ground-state masses used as input to the focal-plane fits. Although most of the masses have been remeasured to higher precision since the 2003 Atomic Mass Evaluation [14], only the changes in the masses of ^{32}S and ^{36}K are large enough to be significant to the present work.

Nuclide	Mass (u)	Ref.
^3H	3.0160492777(25)	[14]
^3He	3.0160293191(26)	[14]
^{20}Ne	19.9924401754(19)	[14]
^{24}Mg	23.985041700(14)	[14]
^{28}Si	27.9769265325(19)	[14]
^{32}S	31.9720711735(16)	[37]
^{36}Ar	35.967545106(29)	[14]
^{36}K	35.98130226(42)	[38]

indicate. Ultimately, an uncertainty of 300 eV per target was assigned, which is a conservative compromise. The areal density of implanted material was known for each target [26] and accounted for. Based on the symmetric method of target preparation, we do not expect significant asymmetries in the depth profile of implanted material.

In category II are uncertainties associated with counting statistics, beam energy, beam position on target (i.e., the shifting procedure), and triton angular distributions. Counting statistics contributed < 300 eV of uncertainty to each measurement at 10° and < 1.2 keV at 20° . The focal-plane fits contributed an additional uncertainty that was < 100 eV at both angles. The beam energy was determined to roughly 3 keV by an analyzing magnet following the tandem. It was therefore assumed that the beam energy could vary randomly and uniformly within a 6-keV range over the course of the experiment. Between 4 and 13 runs were taken at effectively randomly distributed times for each target at each angle during the experiment and therefore the average beam energy for each target was expected to be relatively close to the common central value of 32000.0 keV. The rms deviation from this central value [39] for each target at each angle was calculated under these assumptions and ranged between 480 and 866 eV, yielding total uncertainties between 728 and 1060 eV per measurement. The uncertainty in the shifting procedure that accounted for drifts in beam position was 290 eV per spectrum, or 410 eV per measurement. Finally, an uncertainty was approximated for the possible effects of angular distributions on the peak centroids due to the finite size of the entrance aperture to the spectrograph. The spectrograph was set to focus on the $^{28}\text{Si}(^3\text{He}, t)^{28}\text{P}$ reaction so that reactions on all targets would be measured with identical settings. This resulted in kinematic broadening of peaks that was largest and second largest for the $A = 20, 36$ reactions, respectively. The widths of peaks in the $A = 20, 36$ cases were measured, and the data were combined to increase the sample size. The average contribution from kinematic broadening to the FWHM of peaks at 10° and 20° of 3.9 and 7.7 keV, respectively, was deduced by comparing it with the $A = 28$ case. A rough upper limit on the magnitudes of the centroid shifts was determined by assuming that all counts contributing to broadening on one side of the peak were from a particular half of the entrance aperture to the spectrometer. Then it was approximated that the differential cross section varies by a maximal factor of 2.4 from one edge of the entrance aperture to the other based on the steepest measured angular distributions from the $^{28}\text{Si}(^3\text{He}, t)^{28}\text{P}$ [40] and $^{32}\text{S}(^3\text{He}, t)^{32}\text{Cl}$ [41] reactions at 35 and 34.5 MeV, respectively. Under these assumptions, an anisotropic angular distribution would contribute more counts to one side of the nominal centroid from an isotropic distribution than to the other side, causing a shift in the centroid. In this worst case, the peak centroid could shift by as much as 547 eV at 10° and 1094 eV at 20° . Respective 1σ uncertainties of 316 and 632 eV were approximated by assuming that the worst-case values are the limits of a uniform probability density function (PDF). Uncertainties of this magnitude were applied to the ^{36}Ar calibrations, because both peaks used corresponded to levels with the same spin and the effects of their angular distributions are unlikely to cancel with each other. In the case of ^{32}Cl , half

TABLE III. Standard-deviation uncertainties in the measured masses of ^{20}Na , ^{24}Al , ^{28}P , and ^{32}Cl (eV). Categories I and II are defined in the text.

Effect	Category	^{20}Na ($10^\circ/20^\circ$)	^{24}Al ($10^\circ/20^\circ$)	^{28}P ($10^\circ/20^\circ$)	^{32}Cl ($10^\circ/20^\circ$)
Mass excess of ^{36}K	I	390/390	390/390	390/390	390/390
Excitation energies in ^{36}K	I	382/382	382/382	382/382	382/382
Excitation energies in nuclide of interest	I	36/36	55/55	100/100	200/200
Target thickness	I	424/424	424/424	424/424	424/424
Statistics in ^{36}K spectrum	II	191/875	191/875	191/875	191/875
Statistics in spectrum of interest	II	154/299	122/386	94/167	188/745
Focal-plane fit	II	41/43	41/43	42/43	87/94
Shifting procedure	II	410/410	410/410	410/410	410/410
Beam energy	II	987/778	935/812	1060/911	935/728
Angular distributions	II	316/632	316/632	316/632	353/706
Total for each angle	I and II	1335/1584	1295/1620	1388/1637	1328/1745
Total for recommended value	I and II	1128	1117	1164	1163

of this uncertainty was added, because it is closer to $A = 28$ and the expected broadening was milder for the single peak used. In the case of ^{28}P , no additional uncertainty was added, because the peaks were in focus. No additional uncertainty was added for ^{24}Al or ^{20}Ne either, because four or more peaks were used in each of these cases and we expect the randomized effects of their individual angular distributions to cancel to a large extent. The residuals in the focal-plane fits indicate that these uncertainty estimates for angular distribution effects are conservative.

To determine the uncertainty in the measurements at each individual angle, all of the contributing uncertainties were added in quadrature. To combine the measurements at 10° and 20° and determine a total uncertainty for each mass, those in category I were subtracted out in quadrature at each angle leaving only uncertainties in category II, which were treated as 1σ limits of Gaussian PDFs. These PDFs were combined to produce a weighted average of each mass value, with a reduced total uncertainty. The uncertainties in category I were then added back in quadrature to yield a final 1σ mass-excess uncertainty of 1.1 or 1.2 keV. The uncertainties are summarized in Table III.

IV. RESULTS AND DISCUSSION

Table IV is a summary of the measured mass excesses for each nuclide as measured at each angle, and the recommended overall mass excess for each nuclide based on the combination of both measurements. We proceed by discussing the results for ^{32}Cl , ^{28}P , ^{24}Al , and ^{20}Na individually.

A. Mass of ^{32}Cl

We measure the mass excess of ^{32}Cl to be $-13333.8(12)$ keV. This is consistent with, and more precise than, the AME03 [14] value of $-13330(7)$ keV. The AME03 [14] value is based on two measurements of the $^{32}\text{S}(p,n)^{32}\text{Cl}$ reaction threshold [15,16] and a measurement of the $^{32}\text{S}(^3\text{He},t)^{32}\text{Cl}$ reaction Q value [41]. The present value may also be compared with the more recent value of $-13337.0(16)$ keV that was determined [2] by combining the

^{31}S mass from AME03 [14] with a new ^{32}Cl proton-separation energy from precision ^{32}Ar β -delayed proton- [1,6] and γ - [2] decay measurements. The present value is 3.2 keV (1.6σ) higher than the value from Ref. [2].

The new ^{32}Cl mass may be used together with the excitation energy of $5046.3(4)$ keV [2] for the lowest $T = 2$ ^{32}Cl level to calculate a new value for the latter's mass excess of $-8287.5(12)$ keV. This value is 4.0 keV higher than the currently employed value of $-8291.5(18)$ keV [2,4], which is based on the AME03 [14] mass of ^{31}S . The present value may, in turn, be combined with the measured mass of ^{32}Ar [3] to calculate a new value of $Q_{\text{EC}} = 6087.3(22)$ keV for the superallowed β decay of ^{32}Ar . This is 4.0 keV lower than the currently employed value of $6091.3(25)$ keV [2] (also based on ^{31}S from AME03 [14]).³ The uncertainty in Q_{EC} is now limited by the 1.8-keV uncertainty in the mass excess of ^{32}Ar .

The new mass for the lowest $T = 2$ level in ^{32}Cl yields a substantial improvement in three areas: the $e^+ - \nu_e$ correlation in the superallowed β decay of ^{32}Ar , the isospin-symmetry-breaking correction to the ft value for this decay, and the most precise test of the isobaric multiplet mass equation (IMME) [42–44].

The change in Q_{EC} shifts the β - ν correlation coefficient for ^{32}Ar decay, which was initially deduced to be $0.9989 \pm 0.0052(\text{stat}) \pm 0.0039(\text{syst})$ [1]. The variation in \tilde{a} with respect to Q_{EC} was determined in Ref. [1] to be $-1.2 \times 10^{-3} \text{ keV}^{-1}$. We measure Q_{EC} to have shifted by -4.0 keV, so \tilde{a} must be adjusted by $+0.0048$ to account for the present result. Considering the magnitudes of the original uncertainties assigned to \tilde{a} , an adjustment of 0.0048 significantly changes the associated constraints on the potential contributions of scalar currents to the β decay of ^{32}Ar . The experiment of Ref. [1] is currently being reanalyzed to provide a new value

³The value $Q_{\text{EC}} = 6091.3(25)$ keV was erroneously calculated in Sec. VI A of Ref. [2] because the mass-excess value of $-8291.5(18)$ keV for the lowest $T = 2$ level in ^{32}Cl was mistakenly adopted from Ref. [4]. However, we choose to make comparisons to these values because they are the most recent ones used to calculate \tilde{a} and δ_C^{exp} .

TABLE IV. Ground-state mass excesses (keV) measured in the present work compared with the corresponding values from the 2003 Atomic Mass Evaluation (AME03) [14]. The second and third columns show the mass excesses measured at 10° and 20° , respectively. The fourth column shows the two results combined into a single recommended value as discussed in the text. The fifth column shows the corresponding value from AME03. The sixth and seventh columns show the difference between the recommended mass excess and the corresponding value from AME03 in units of keV and standard deviations, respectively.

Nuclide	M.E. (10°)	M.E. (20°)	M.E. (recommended)	M.E. [14]	Difference (keV)	Difference (σ)
^{20}Na	6850.7(13)	6851.0(16)	6850.8(11)	6848(7)	+2.8(71)	+0.4
^{24}Al	-48.0(13)	-46.2(16)	-47.4(11)	-56.9(28)	+9.5(30)	+3.2
^{28}P	-7147.7(14)	-7147.2(16)	-7147.5(12)	-7159(3)	+11.5(32)	+3.6
^{32}Cl	-13334.7(13)	-13332.0(17)	-13333.8(12)	-13330(7)	-3.8(71)	-0.6

for \tilde{a} [6]. The reanalysis will incorporate several changes including the present result, and is not finished, so it is not possible to quote a new value for \tilde{a} in the present work.

An experimental value for the isospin-symmetry-breaking correction $\delta_C^{\text{exp}} = 2.1(8)\%$ has already been determined [2] for the superallowed β decay of ^{32}Ar . This value is sensitive to our new result for Q_{EC} , which yields a new value for the statistical rate function of $f = 3494(7)$ [45] [to be compared with the previous value of 3506(8) [2]] and, hence, a new value of $\delta_C^{\text{exp}} = 1.8(8)\%$, which is still in good agreement with the theoretical value of $\delta_C^{\text{th}} = 2.0(4)\%$ [2]. Uncertainties in the superallowed branching, half-life, and mass of ^{32}Ar (in order of importance) must now be reduced to decrease the uncertainty in δ_C^{exp} .

The most stringent test of the IMME is presently the lowest $T = 2$ quintet in the $A = 32$ system [46]. Data on this multiplet have been improved substantially in recent years [3,46,47]. Further gains could be achieved by improving the precision of the ^{32}Cl and ^{32}Ar members. The present measurement improves and changes the mass of the ^{32}Cl level substantially. To test the quadratic IMME, we applied a cubic IMME fit to the best data available on this multiplet together with our new value for ^{32}Cl . The fit yields an excellent $\chi^2/\nu = 0.44/1$, and a cubic coefficient that is inconsistent with zero by 7.9σ . This confirms the breakdown of the quadratic IMME observed in Ref. [46] and shows that it was not due to an erroneous mass value for ^{32}Cl as speculated [46]. Our results in combination with Refs. [1,2,6] imply that the AME03 [14] recommendation for the mass of ^{31}S may be inaccurate. We reserve a more detailed presentation of the IMME reevaluation for another paper [5], which will report a precise direct measurement of the ^{31}S mass.

B. Mass of ^{28}P

We measure the mass excess of ^{28}P to be $-7147.5(12)$ keV. This is 11.5 keV higher than the AME03 [14] value of $-7159(3)$ keV. These two values are mutually inconsistent by 3.6σ . The AME03 [14] value is based on measurements of the $^{28}\text{Si}(p,n)^{28}\text{P}$ reaction threshold [15,16]. In the AME03 [14], the original values have undergone recalibrations that are not transparent. A recent independent reevaluation [19] of the same measurements yielded an average value of $-7152.9(33)$ keV, which is only 1.5σ away from the present value.

We use our measurement to calculate a new value for the proton-separation energy $S_p(^{28}\text{P}) = 2052.2(12)$ keV, where the mass values of ^{27}Si and ^1H have been adopted from AME03 [14]. Adding this value to the c.m. energy of 3835(20) keV [48] for the β -delayed proton decay of the lowest $T = 2$ level in ^{28}P yields a new excitation energy of 5887(20) keV for this level that may be compared with the currently accepted value of 5900(21) keV [48].

C. Mass of ^{24}Al

We measure the mass excess of ^{24}Al to be $-47.4(11)$ keV. This is 9.5 keV higher than the AME03 [14] value of $-56.9(28)$ keV. These two values are mutually inconsistent by 3.2σ . The AME03 [14] mass is based on a single measurement [15] of the $^{24}\text{Mg}(p,n)^{24}\text{Al}$ reaction threshold. Similar to the case of ^{28}P , a recalibration of this original measurement was made in AME03 [14]. A recent independent recalibration of the same measurement [19] yielded a value of $-47.4(26)$ keV, in excellent agreement with the present value.

We use our measurement to calculate a new value for the proton-separation energy $S_p(^{24}\text{Al}) = 1863.0(14)$ keV, where the mass values of ^{23}Mg [49] and ^1H [14] have been adopted. We have compiled available data [50–52] to produce an average value for the c.m. energy of 4084.0(32) keV for the β -delayed proton decay of the lowest $T = 2$ level in ^{24}Al . Adding this value to S_p yields a new excitation energy of 5947.0(35) keV for the $T = 2$ level: somewhat lower and more precise than the previously accepted value of 5957(6) keV [27].

The new value for S_p resolves the discrepancy in the energy of the lowest proton resonance in the $^{23}\text{Mg}(p,\gamma)^{24}\text{Al}$ reaction [19–21] and also constrains the measurement of the resonance strength, which is tied to the energy. This topic will be explored in a subsequent publication [53] that will focus on the astrophysical implications of the present measurements; it will also include new data on the excitation energies of proton-unbound levels in ^{32}Cl and ^{36}K .

D. Mass of ^{20}Na

We measure the mass excess of ^{20}Na to be 6850.8(11) keV. This is consistent with, and more precise than, the AME03 [14] value of 6848(7) keV. The AME03 [14] value is based on a measurement of the $^{20}\text{Ne}(p,n)^{20}\text{Na}$ reaction threshold [17].

We use our measurement to calculate a new value for the proton-separation energy $S_p(^{20}\text{Na}) = 2190.1(11)$ keV, where the mass values of ^{19}Ne [54] and ^1H [14] have been adopted. We have compiled available data [30,55,56] to produce an average value for the c.m. energy of 4335(12) keV for the β -delayed proton decay of the lowest $T = 2$ level in ^{20}Na . Adding this value to S_p yields a new excitation energy of 6525(12) keV for the $T = 2$ level that may be compared with the previously accepted value of 6534(13) keV [29].

V. CONCLUSIONS AND OUTLOOK

The ground-state mass excesses of ^{20}Na and ^{24}Al have been measured to a precision of 1.1 keV, and those of ^{28}P and ^{32}Cl to a precision of 1.2 keV: substantial improvements over previous measurements. Major deviations from the 2003 Atomic Mass Evaluation [14] are found in the cases of ^{24}Al and ^{28}P .

The mass excess of the lowest $T = 2$ level in ^{32}Cl has been determined to a precision of 1.2 keV by adding the well-known excitation energy to the presently measured ground-state mass excess. It is now possible to determine the mass excesses of the lowest $T = 2$ levels in ^{20}Na , ^{24}Al , and ^{28}P in the same way by measuring the delayed γ rays from the superallowed $0^+ \rightarrow 0^+$ β decays of ^{20}Mg , ^{24}Si , and ^{28}S and adding the resulting

excitation energies in ^{20}Na , ^{24}Al , and ^{28}P to the corresponding ground-state mass excesses from the present work.

The present experimental method could be generalized to other cases and refined to a few hundred eV in precision by implanting $N > 1$ species of ions in the same carbon foil with $M < N$ species serving as calibrants. Doing so would effectively eliminate systematic uncertainties related to target thickness and drifts in beam position and energy as demonstrated in a recent precision measurement of the ^{46}V β -decay Q value [24].

ACKNOWLEDGMENTS

We gratefully acknowledge the contributions of the accelerator operators at MLL and WNSL. We thank K. Deryckx, B. M. Freeman, G. C. Harper, A. Palmer, D. Seiler, D. A. Short, and D. I. Will for contributing to the preparation of the ion-implanted targets, C. Ugalde for providing the ^{20}Ne target used at WNSL, and P. D. Parker for contributing to the measurements at WNSL and useful comments on the manuscript. This work was supported by the United States Department of Energy under Contract Nos. DE-FG02-91ER40609 and DE-FG02-97ER41020, and the DFG Cluster of Excellence ‘‘Origin and Structure of the Universe’’ (www.universe-cluster.de).

-
- [1] E. G. Adelberger *et al.*, *Phys. Rev. Lett.* **83**, 1299 (1999).
 - [2] M. Bhattacharya *et al.*, *Phys. Rev. C* **77**, 065503 (2008).
 - [3] K. Blaum, G. Audi, D. Beck, G. Bollen, F. Herfurth, A. Kellerbauer, H.-J. Kluge, E. Sauvan, and S. Schwarz, *Phys. Rev. Lett.* **91**, 260801 (2003).
 - [4] M. C. Pyle *et al.*, *Phys. Rev. Lett.* **88**, 122501 (2002).
 - [5] CPT Collaboration (in preparation); C. Wrede *et al.*, [<http://meetings.aps.org/Meeting/HAW09/Event/110401>].
 - [6] A. García *et al.* (in preparation).
 - [7] A. Gorelov *et al.*, *Phys. Rev. Lett.* **94**, 142501 (2005).
 - [8] J. C. Hardy and I. S. Towner, *Phys. Rev. C* **79**, 055502 (2009).
 - [9] I. S. Towner and J. C. Hardy, *Phys. Rev. C* **77**, 025501 (2008).
 - [10] G. A. Miller and A. Schwenk, *Phys. Rev. C* **78**, 035501 (2008).
 - [11] G. A. Miller and A. Schwenk, *Phys. Rev. C* **80**, 064319 (2009).
 - [12] H. Liang, N. V. Giai, and J. Meng, *Phys. Rev. C* **79**, 064316 (2009).
 - [13] N. Auerbach, *Phys. Rev. C* **79**, 035502 (2009).
 - [14] G. Audi, A. H. Wapstra, and C. Thibault, *Nucl. Phys. A* **729**, 337 (2003).
 - [15] J. C. Overley, P. D. Parker, and D. A. Bromley, *Nucl. Instrum. Methods* **68**, 61 (1969).
 - [16] D. R. Goosman, K. W. Jones, E. K. Warburton, and D. E. Alburger, *Phys. Rev. C* **4**, 1800 (1971).
 - [17] D. H. Wilkinson, D. E. Alburger, D. R. Goosman, K. W. Jones, E. K. Warburton, G. T. Garvey, and R. L. Williams, *Nucl. Phys. A* **166**, 661 (1971).
 - [18] J. M. Freeman, *Nucl. Instrum. Methods* **134**, 153 (1976).
 - [19] L. Erikson *et al.*, *Phys. Rev. C* **81**, 045808 (2010).
 - [20] D. W. Visser, C. Wrede, J. A. Caggiano, J. A. Clark, C. Deibel, R. Lewis, A. Parikh, and P. D. Parker, *Phys. Rev. C* **76**, 065803 (2007).
 - [21] G. Lotay *et al.*, *Phys. Rev. C* **77**, 042802(R) (2008).
 - [22] R. Hertenberger *et al.*, *Nucl. Instrum. Methods A* **536**, 266 (2005).
 - [23] H.-F. Wirth, H. Angerer, T. von Egidy, Y. Eisermann, G. Graw, and R. Hertenberger, Annual Report, Maier-Leibnitz-Laboratorium, 2000 (unpublished).
 - [24] T. Faestermann, R. Hertenberger, H.-F. Wirth, R. Krücken, M. Mahgoub, and P. Maier-Komor, *Eur. Phys. J. A* **42**, 339 (2009).
 - [25] H. J. Scheerer, H. Vonach, M. Löffler, A. v. d. Decken, M. Goldschmidt, C. A. Wiedner, and H. A. Enge, *Nucl. Instrum. Methods* **136**, 213 (1976).
 - [26] C. Wrede, K. Deryckx, B. M. Freeman, A. García, G. C. Harper, A. Palmer, D. A. Short, and D. I. Will (in preparation).
 - [27] P. M. Endt, *Nucl. Phys. A* **521**, 1 (1990).
 - [28] D. Seweryniak *et al.*, *Phys. Lett. B* **590**, 170 (2004).
 - [29] D. R. Tilley, C. M. Cheves, J. H. Kelley, S. Raman, and H. R. Weller, *Nucl. Phys. A* **636**, 249 (1998).
 - [30] A. Piechaczek *et al.*, *Nucl. Phys. A* **584**, 509 (1995).
 - [31] J. Honkanen, M. Kortelahti, J. Äystö, K. Eskola, and A. Hautojärvi, *Phys. Scr.* **19**, 239 (1979).
 - [32] C. E. Moss, N. S. P. King, A. B. Comiter, and R. A. Ristinen, *Nucl. Phys. A* **179**, 89 (1972).
 - [33] T. Björnstad *et al.*, *Nucl. Phys. A* **443**, 283 (1985).
 - [34] W. Trinder *et al.*, *Phys. Lett. B* **348**, 331 (1995).
 - [35] W. Trinder *et al.*, *Nucl. Phys. A* **620**, 191 (1997).
 - [36] M. J. López Jiménez *et al.*, *Eur. Phys. J. A* **10**, 119 (2001).
 - [37] W. Shi, M. Redshaw, and E. G. Myers, *Phys. Rev. A* **72**, 022510 (2005).
 - [38] C. Yazidjian *et al.*, *Phys. Rev. C* **76**, 024308 (2007).
 - [39] C. Amsler *et al.*, *Phys. Lett. B* **667**, 1 (2008).
 - [40] B. Ramstein, L. H. Rosier, and C. Jeanperrin, *Nucl. Phys. A* **317**, 460 (1979).

- [41] C. Jeanperrin, L. H. Rosier, B. Ramstein, and E. I. Obiajunwa, *Nucl. Phys. A* **503**, 77 (1989).
- [42] E. P. Wigner, in *Proceedings of the Robert A. Welch Foundation Conference on Chemical Research, Houston*, edited by W. O. Millikan (Robert A. Welch Foundation, Houston, 1957), Vol. 1.
- [43] S. Weinberg and S. B. Treiman, *Phys. Rev.* **116**, 465 (1959).
- [44] J. Britz, A. Pape, and M. S. Antony, *At. Data Nucl. Data Tables* **69**, 125 (1998).
- [45] I. S. Towner (private communication).
- [46] A. A. Kwiatkowski *et al.*, *Phys. Rev. C* **80**, 051302(R) (2009).
- [47] S. Triambak *et al.*, *Phys. Rev. C* **73**, 054313 (2006).
- [48] F. Pougheon *et al.*, *Nucl. Phys. A* **500**, 287 (1989).
- [49] A. Saastamoinen *et al.*, *Phys. Rev. C* **80**, 044330 (2009).
- [50] J. Äystö, D. M. Moltz, M. D. Cable, R. D. von Dincklage, R. F. Parry, J. M. Wouters, and J. Cerny, *Phys. Lett. B* **82**, 43 (1979).
- [51] A. G. Ledebuhr, L. H. Harwood, R. G. H. Robertson, and T. J. Bowles, *Phys. Rev. C* **22**, 1723 (1980).
- [52] Y. Ichikawa *et al.*, *Phys. Rev. C* **80**, 044302 (2009).
- [53] C. Wrede *et al.* (in preparation).
- [54] W. Geithner *et al.*, *Phys. Rev. Lett.* **101**, 252502 (2008).
- [55] D. M. Moltz, J. Äystö, M. D. Cable, R. D. von Dincklage, R. F. Parry, J. M. Wouters, and J. Cerny, *Phys. Rev. Lett.* **42**, 43 (1979).
- [56] J. Görres and M. Wiescher, *Phys. Rev. C* **52**, 412 (1995).